Proceedings of the
Annual Stability Conference
Structural Stability Research Council
Pittsburgh, Pennsylvania, May 10-14, 2011

Buckling, Post-Buckling and Strength of Cruciform Columns

P.B. Dinis[1], D. Camotim[1]

Abstract

This paper presents and discusses the results of a numerical investigation on the buckling, post-buckling and strength behavior of short-to-intermediate cruciform steel columns with pinned and fixed supports. Most of these results were obtained through ABAQUS shell finite element analyses – to shed new light on the column buckling behavior, some GBT-based analyses are also carried out. The shell finite element results displayed consist of (i) elastic and elastic-plastic post-buckling equilibrium paths, and (ii) curves and diagrams showing the evolution, along a given path, of column deformations, normal stresses and plastic strains. The ultimate strengths obtained, together with a few experimental values reported in the literature, are used to assess whether the current Direct Strength Method design curves can estimate the cruciform column strength adequately. Also included is a brief comparison between the post-buckling and strength behaviors of equal-leg angle and cruciform columns – the original motivation of this work.

1. Introduction

It is well known that thin-walled members having cross-sections with all their wall mid-lines intersecting at a single point (*e.g.*, angle, T-section and cruciform members) exhibit no primary warping – the cross-section warping resistance stems solely from secondary warping. This feature automatically implies an extremely low torsional stiffness, thus rendering those thin-walled members highly susceptible to the occurrence of buckling phenomena involving cross-section torsion, namely torsional, local-torsional or flexural-torsional buckling. Moreover, in members with the above cross-section shapes and equal legs it is often quite hard to separate the torsional and local deformations and, therefore, to distinguish between local and torsional (global) buckling – such members commonly exhibit "mixed" local/torsional buckling mode shapes. In other words, it is by no means a straightforward task to assess the buckling mode nature (local or global) in equal-leg angle, T-section and cruciform members with short-to-intermediate lengths. As these two instability phenomena are associated with markedly different post-critical behaviors (strength reserves), it is fair to say that this knowledge may have far-reaching implications on the definition of a structural model or design approach capable of providing accurate ultimate strength estimates for such members.

The structural behavior and design of angle (mostly), T-section and cruciform members has attracted the attention of several researchers in the past (*e.g.,* Kitipornchai & Chan 1987, Dabrowski 1988, Kitipornchai *et al.* 1990, Chen & Trahair 1994, Popovic *et al.* 1999, 2001). More recently, Trahair

[1] Department of Civil Engineering and Architecture, ICIST/IST, Technical University of Lisbon, Lisbon, Portugal. dinis@civil.ist.utl.pt and dcamotim@civil.ist.utl.pt

(2003, 2005), Rasmussen (2005, 2006), Young (2004), Mohan *et al.* (2005), Ellobody & Young (2005), Young & Ellobody (2007) and Chodraui *et al.* (2007) devoted a fair amount of work to investigate the buckling, post-buckling and strength behavior of angle members, with the objective of improving the available design rules to predict their ultimate strength (adopting local buckling concepts). Moreover, a recent numerical investigation by Dinis *et al.* (2008, 2010b), involving GBT (Generalized Beam Theory) buckling analyses, shed some new light on how to characterize and/or distinguish local and global buckling modes in angle, T-section and cruciform thin-walled members (columns, beams and beam-columns). On the basis of the results obtained, the authors concluded that there is a need for a specific design curve to estimate the ultimate strength of equal-leg angle columns, and that it should be based on torsional (global), instead of local, buckling concepts. Some initial steps were already taken towards achieving this goal, namely the analysis of the post-buckling and strength of several short-to intermediate angle columns with pinned and fixed end supports (Dinis *et al.* 2010a). This last investigation revealed that short-to-intermediate equal-leg angle columns, which have almost identical critical buckling loads/stresses, exhibit (i) a wide spectrum of elastic post-critical strengths, ranging from "pure local" (high) to "pure global" (low) and (ii) several surprising behavioral features stemming from the occurrence of significant corner (shear centre) flexural displacements, due to the absence of cross-section double symmetry – they provide a logical explanation for the differences between the displacements and stress distributions associated with the various column post-buckling behaviors, some of which were found to be quite unexpected.

In order to confirm and/or complement the above findings, it was decided to investigate the structural behavior of cruciform columns – due to the cross-section double symmetry (coincident centroid and shear center), no corner flexural displacements should occur, which means that each of the four legs are expected to behave identically. Thus, the aim of this work is to present and discuss numerical (shell finite element) results concerning the buckling, post-buckling (elastic and elastic-plastic) and ultimate strength of equal-leg cruciform columns. Such numerical results, obtained from ABAQUS (Simulia 2008) analyses, concern pinned and fixed steel ($E=210GPa$ and $\nu=0.3$) columns with typical cross-section dimensions (four plates with width $b=80mm$ and thickness $t=4mm$), short-to-intermediate lengths and various yield-to-critical stress ratios. All the columns analyzed contain critical-mode geometrical imperfections with small amplitudes (*10%* of the wall thickness t) and no residual stresses. The columns are discretized into fine 4-node isoparametric S4 shell elements (length-to-width ratio close to *1*), the end supports are modeled by imposing either null transverse displacements at all end section nodes (pinned supports – P condition) or by attaching rigid end-plates to the end section centroids (fixed supports – F condition), and the axial compression is simulated through compressive forces uniformly distributed along both column end-section mid-lines. Detailed accounts of all column finite element modeling issues can be found in Dinis & Camotim (2006) or Dinis *et al.* (2007). In order to characterize the cruciform column buckling behavior, GBT analyses are also performed.

The results displayed consist of (i) elastic and elastic-plastic post-buckling equilibrium paths, and (ii) curves and/or diagrams providing the evolution, along a given equilibrium path, of the column deformed configuration and the longitudinal normal stresses acting along the mid-line of several cross-sections. The elastic-plastic ultimate strength data obtained, together with experimental values reported in the literature (Nishimo *et al.* 1968, Rasmussen & Hancock 1992), are employed to assess whether the current Direct Strength Method (DSM – *e.g.*, Schafer 2008) design curves are able to estimate the strength of cruciform columns adequately. Finally, the paper also includes a brief comparison between the post-buckling and strength behaviors of equal-leg angle and cruciform columns – the original motivation of this work. A more detailed, mechanically-based comparison is under preparation and will be reported in the near future.

2. Buckling Behavior – Column Length Selection

The curves in Fig. 1(a) show the variation of the ABAQUS critical load P_{cr} with the column length L (logarithmic scale), both for pinned (P curve) and fixed (F curve) cruciform columns[2] – it also depicts single half-wave buckling loads $P_{b.1}$ yielded by GBT analyses including *11* deformation modes: *4* global (**1**-**4**) and *7* local (**5**-**11**). As for Figs. 1(b_1)-(b_2), they display the GBT modal participation diagrams for columns with both end support conditions – they provide the contributions of each GBT deformation mode to the column buckling modes. Finally, Fig. 1(c) shows the GBT-based buckling mode shapes of the P columns with *L=20*, *200*, *1000cm*, as well as the in-plane shapes of the first *8* deformation modes (axial extension excluded). The observation of these buckling results prompts the following remarks:

(i) Both the pinned and fixed columns exhibit similar buckling features (obviously, the fixed P_{cr} values are generally higher than their pinned counterparts): (i_1) P_{cr} decreases monotonically with L and corresponds to single half-wave buckling (similar curves for columns having cross-sections with wall mid-lines not intersecting at a point always exhibit local minima associated with local and/or distortional buckling in growing half-wave numbers), (i_2) the GBT and ABAQUS results virtually coincide, and (i_3) the torsion mode **4** plays a key role, as it participates in the critical buckling modes of all but the very long columns.

(ii) For the entire length range, the critical buckling modes of all pinned and fixed columns involve just three deformation modes (**2/3**, **4**, **6**) – note that (ii_1) modes **2** and **3** (minor/major axis flexure) are basically the same and (ii_2) the participation of (local) mode **6** is similar in both P and F columns. For very short columns, buckling takes place in mixed local-torsional modes (**4+6**), with a dominant contribution from mode **4**. Short-to-intermediate columns buckle in pure torsional modes (**4**), while the longer ones buckle in pure flexural modes (**2/3**).

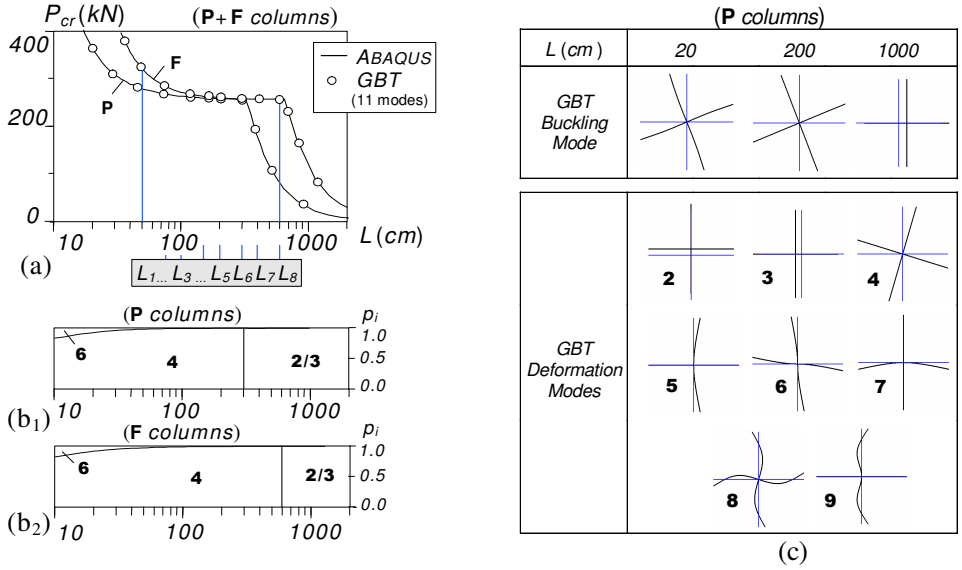

Figure 1: Pinned and fixed column (a) P_{cr} vs. L curves, and (b) GBT modal participation diagrams, and (c) *3* pinned column buckling modes and *8* GBT deformations mode shapes.

[2] At this stage, it is worth noting that buckling results were obtained for a third end support condition, often termed "simply supported" in the literature: the column end cross-sections are attached to rigid end-plates (through their centroids), which are (i) free to exhibit flexural (global) rotations and (ii) restrained against torsional rotation – in an experimental test, this would corresponds to having the rigid end-plates resting on spherical hinges that are partially "inserted" in them (in order to prevent the torsional rotations). It was found that the buckling behavior of the short-to-intermediate columns with the above end support conditions virtually coincides with that exhibited by the fixed columns dealt with in this work.

(iii) In order to study the short-to-intermediate column post-buckling behavior, the eight lengths shown in Fig. 1(a) were selected. They concern columns (iii_1) buckling in the P_{cr} *vs.* L curve "horizontal plateaus" (pure torsional modes) and (iii_2) with very similar mid-span cross-section buckled shapes – see Fig. 1(c), concerning pinned columns. The lengths selected are L_1=*50cm*, L_2=*75cm*, L_3=*100cm*, L_4=*150cm*, L_5=*200cm*, L_6=*300cm*, L_7=*400cm*, L_8=*600cm* – six pinned (L_1-L_6 – $218.2 \geq \sigma_{cr} \geq 201.1 MPa$) and six fixed ($L_3$-$L_8$ – $212.2 \geq \sigma_{cr} \geq 200.9 MPa$) columns were analyzed.

3. Column Post-Buckling Behavior

ABAQUS shell finite element analyses are used to study the post-buckling behavior of columns containing critical-mode initial imperfections with small amplitudes (*10%* of the wall thickness t=*4mm* – torsional modes with mid-span rigid-body rotation β_0=*0.005 rad*). The columns analyzed have (i) pinned or fixed end sections, (ii) the short-to-intermediate lengths indicated before and (iii) *7* yield-to-critical stress ratios: $f_y/\sigma_{cr.Av} \approx$ *1.2*, *1.8*, *2.6*, *4.0*, *6.0*, *9.0*, ∞, values related to the "average" critical stress $\sigma_{cr.Av}$=*201 MPa* (the "plateau" critical stresses are not fully identical) – the elastic behavior is associated with $f_y = \infty$.

3.1 Elastic Post-Buckling Behavior

Figs. 2(a)-(b) show the upper parts of the post-buckling equilibrium paths P/P_{cr} *vs.* β, where β is the mid-span chord rigid-body rotation, for (i) pinned cruciform columns (P columns) with lengths L_1 to L_6 and (ii) fixed cruciform columns (F columns) with lengths L_3 to L_8 – also shown are the L_5 pinned and the L_7 fixed column mid-span cross-section deformed configurations at β=*0.4 rad*. The observation of these elastic post-buckling results leads to the following remarks:

(i) The pinned and fixed column post-buckling behaviors (equilibrium paths) exhibit similar characteristics: both (i_1) are clearly stable (fairly high post-critical strength), (i_2) have a post-critical stiffness that decreases with the column length and (i_3) only involve cross-section rigid-body rotations (no cross-section shear centre displacements occur – see the two column mid-span cross-section deformed configurations).

(ii) The fixed column post-critical stiffness values are a bit higher than those exhibited by the pinned columns. Since the difference stems from the end section warping and rotation restraints, the small stiffness increase confirms the small impact of those restrictions on the buckling behavior of cruciform columns with short-to-intermediate lengths.

(iii) The P and F column post-buckling behavior described above is similar to that recently unveiled for pinned and fixed angle columns, when the shear centre displacement is fully restrained (Dinis *et al.* 2010a). This statement can be clearly confirmed by looking at Figs. 3(a)-(b), which show the P/P_{cr} *vs.* β equilibrium paths for (iii_1) the L_5 pinned and L_7 fixed cruciform columns (curves already

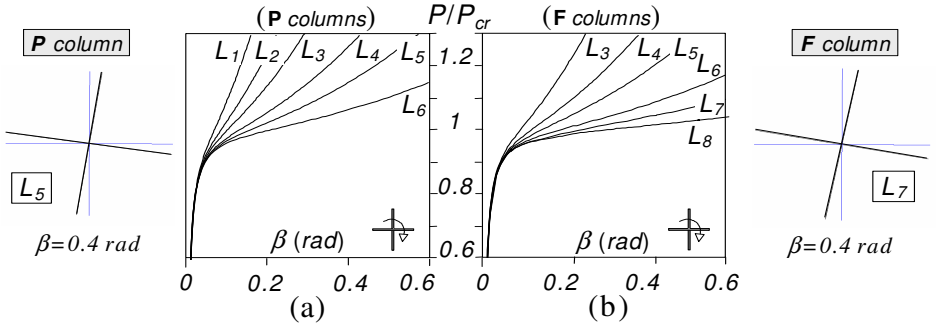

Figure 2: (a) Pinned and (b) fixed P/P_{cr} *vs.* β column equilibrium paths and L_5 and L_7 column mid-span cross-section deformed configurations.

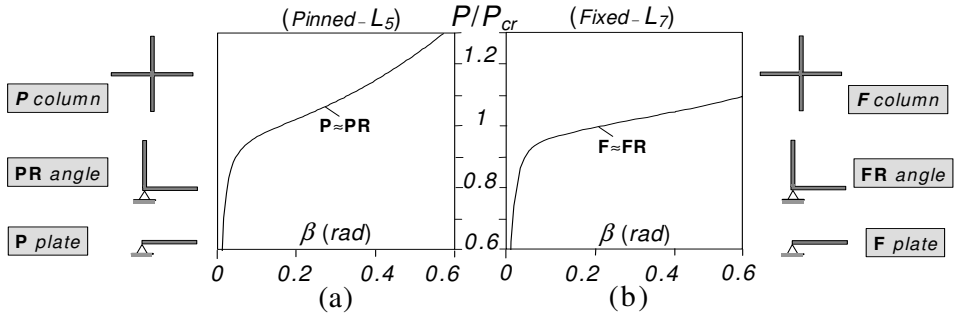

Figure 3: P/P_{cr} *vs.* β equilibrium paths: (a) P plate, PR angle, P column (L_5), and (b) F plate, FR angle, F column (L_7).

plotted in Figs. 2(a)-(b)), and (iii$_2$) equal-leg angle columns with the same dimensions (*80×80×4mm* and L_5 or L_7 lengths), but the shear centre displacement fully restrained (PR and FR angle columns). For comparison purposes, isolated plates with the same dimensions, one longitudinal free edge and (iii$_1$) the remaining ones pinned (P plate) or (iii$_2$) one longitudinal pinned and both transverse edges fixed (F plate) were also analyzed. The observation of these three sets of post-buckling equilibrium paths prompts the following comments:

(iii.1) The plates, angle columns with the shear centre displacement fully restrained and cruciform columns share the same critical buckling stresses (differences below *1%*) and post-buckling behaviors. The corresponding P/P_{cr} *vs.* β equilibrium paths, both for pinned and fixed end supports, are impossible to distinguish (virtually identical).

(iii.2) The above coincidence means that each cruciform column leg behaves like a pinned-free (P columns) or a fixed-free (F columns) long plate. This is confirmed by the longitudinal normal stress distributions (σ/σ_{cr}) shown in Figs. 4(a)-(b) – they concern two adjacent legs of the L_5 pinned and L_7 fixed cruciform column mid-span cross-sections. Note that these stress distributions become gradually "less uniform" as post-buckling progresses (see the equilibrium states indicated), with the higher value occurring at the corner. These are precisely the widely known (almost parabolic) shapes of the plate stress distributions – *e.g.*, see Rasmussen (2005).

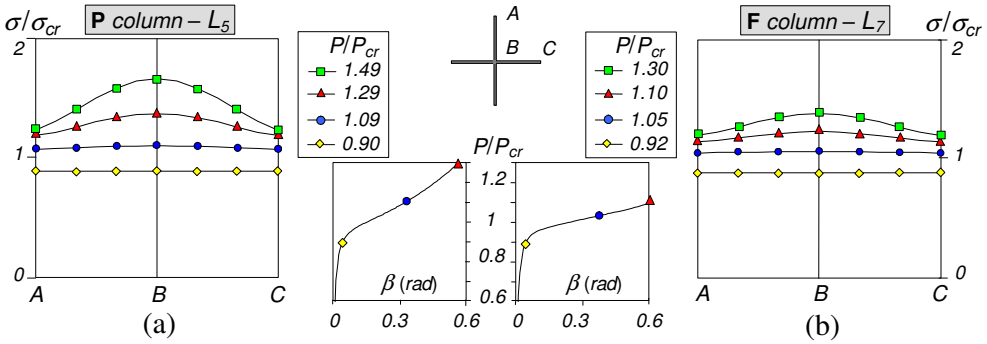

Figure 4: Mid-span longitudinal normal stress distribution evolution of the (a) L_5 P and (b) L_7 F cruciform columns.

3.2 Elastic-Plastic Post-Buckling Behavior and Strength

This section presents and discusses the results dealing with the elastic-plastic behavior and strength of the pinned and fixed short-to-intermediate cruciform columns that were identified earlier. The results concern columns (i) containing critical-mode initial imperfections with *0.1 t* amplitude and (ii) exhibiting six yield-to-critical stress ratios; $f_y/\sigma_{cr.Av}$≈*1.2*, *1.8*, *2.6*, *4.0*, *6.0*, *9.0*, corresponding to f_y=*235*, *355*, *520*, *800*, *1200*, *1800MPa* (the unrealistically high yield stresses are considered to cover a wide slenderness range) and an "average" critical stress $\sigma_{cr.Av}$=*201MPa*. For comparative purposes, some of the elastic results presented earlier are displayed again – those corresponding to $f_y=f_y/\sigma_{cr.Av}=\infty$.

Figs. 5(a)-(b) shows the upper portions ($P/P_{cr.Av}>0.5$) of five sets of equilibrium paths $P/P_{cr.Av}$ *vs.* β and $P/P_{cr.Av}$ *vs.* ε ($\varepsilon=\delta/L$ is the column axial extension, where δ is the column axial shortening[3]), corresponding to the L_1, L_3 and L_5 pinned columns and five f_y/σ_{cr} ratio values. As for Fig. 5(c), it concerns the L_5 column with $f_y/\sigma_{cr}\approx 2.6$ and shows its deformed configuration and plastic strain distribution near collapse. Lastly, Table 1 provides the column ultimate loads (P_u) for all the pinned columns analyzed in this work. After observing these post-buckling results, one is able to draw the following conclusions:

(i) The onset of yielding defines the point of separation between the elastic and elastic-plastic equilibrium paths. The corresponding applied load level is highly dependent on the yield-to-critical stress ratio – for the yield stresses considered, it falls within the interval $0.8<P/P_{cr.Av}<1.8$.

(ii) Looking at Figs. 5(a)-(b) and Table 1, one readily recognizes that the ultimate load P_u remains practically constant as the short-to-intermediate column length changes (increases). This means that P_u is virtually not affected by the amount of cross-section torsional rotation taking place before collapse – note the huge difference between the collapse mid-span rotations concerning columns L_1 and L_5 (see Fig. 5(a)), while their ultimate loads are practically identical (see Table 1). Moreover, this also indicates that failure is essentially governed by the longitudinal normal stresses stemming from the axial compression, which are basically the same for the five columns considered.

(iii) For $f_y/\sigma_{cr.Av}\leq 1.2$, yielding starts when the column still exhibits a fairly uniform longitudinal normal stress distribution, leading to a very "abrupt" collapse (no elastic-plastic strength reserve). For higher yield stresses, the columns exhibit a gradual increase in elastic-plastic strength reserve, as collapse no longer occurs simultaneously with the onset of yielding. Nevertheless, collapse always occurs fairly "suddenly" and none of the columns exhibits a meaningful amount of ductility prior to failure.

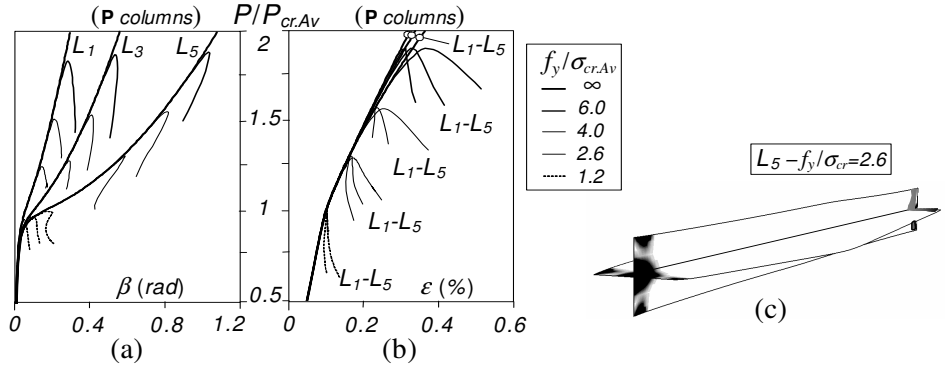

Figure 5: L_1, L_3, L_5 column (a) $P/P_{cr.Av}$ *vs.* β and (b) $P/P_{cr.Av}$ *vs.* ε paths ($5\ f_y/\sigma_{cr.Av}$), and (c) deformed configuration and plastic strains at collapse ($L_5+f_y/\sigma_{cr.Av}\approx 2.6$).

Table 1: Variation of P_u (*kN*) with f_y for pinned columns.

Column	f_y (*MPa*)					
	235	*355*	*520*	*800*	*1200*	*1800*
L_1	*199*	*226*	*260*	*315*	*382*	*452*
L_2	*200*	*227*	*261*	*316*	*382*	*452*
L_3	*200*	*228*	*262*	*316*	*382*	*452*
L_4	*202*	*229*	*263*	*316*	*382*	*452*
L_5	*202*	*229*	*263*	*316*	*382*	*453*
L_6	*203*	*230*	*264*	*317*	*384*	*455*

[3] The column axial shortening is obtained as the average of the sums of the axial displacements occurring at the corresponding nodes of the two column end cross-sections.

(iv) The onset of yielding occurs at the two end sections in all the columns, where (iv_1) the longitudinal normal and shear stresses stemming from the torsional rotation derivative are higher (*e.g.*, Stowell 1951) and (iv_2) non-negligible stress concentrations occur, due to the shell finite element modeling of the pinned supports (*e.g.*, Dinis & Camotim 2006). Collapse is then precipitated by the full yielding of both end sections, caused by a combination of the above two factors and leading to the formation of "torsional plastic hinges". When the ultimate load is reached, practically the whole column volume is still in the elastic range – see the plastic strain distribution depicted in Fig. 5(c).

(v) Finally, note that a yield stress increase of *770%* (from *235* to *1800MPa*) causes only a *225%* rise in column strength (from *≈200* to *≈450kN*).

A similar investigation was also carried out for fixed columns. Figs. 6(a)-(b) display the upper parts ($P/P_{cr}>0.5$) of the post-buckling equilibrium paths (i) $P/P_{cr.Av}$ *vs.* β and (ii) $P/P_{cr.Av}$ *vs.* ε, for the L_3, L_5 and L_7 columns with $f_y/\sigma_{cr.Av}\approx 1.2, 2.6, 4.0, 6.0, \infty$ ($\sigma_{cr.Av}=201MPa$). As for Fig. 6(c), it shows the plastic strain evolution and collapse mechanism of the L_5 column with $f_y/\sigma_{cr.Av}\approx 2.6$. All column ultimate loads (P_u) are given in Table 2. The observation of these post-buckling results prompts the following remarks:

(i) First of all, one notices that most fixed columns (except those with a very low yield stress) exhibit (i_1) a non-negligible elastic-plastic strength reserve (load increase after the onset of yielding), (i_2) a fair amount of ductility prior to failure and (i_3) considerably higher ultimate loads than their pinned counterparts – *e.g.*, the ultimate loads of the F and P L_5 columns with $f_y/\sigma_{cr.Av}\approx 2.6$ are *24%* apart. Moreover, all these features increase with $f_y/\sigma_{cr.Av}$ and are more pronounced for $f_y/\sigma_{cr.Av}\geq 2.6$.

(ii) Like in the pinned columns, for $f_y/\sigma_{cr.Av}\leq 1.2$ yielding starts when the longitudinal normal stress distribution is still fairly uniform, leading to very "abrupt" collapses. Moreover, the fixed columns with higher yield stresses also exhibit growing amounts of (ii_1) elastic-plastic strength reserve and (ii_2) ductility prior to failure.

(iii) As depicted in diagram I of Fig. 6(c), the onset of yielding occurs around the ¼ and ¾-span zones of the column central longitudinal edge, where the longitudinal normal and shear stresses caused by the torsional rotation derivative are higher (*e.g.*, Stowell 1951) – note that this derivative is null at the end and mid-span cross-sections[4]. Collapse corresponds to the almost full yielding of the vast majority of the column volume – as shown in diagram II of Fig. 6(c), only the column zones located in the close vicinity of the end and mid-span cross-sections remain elastic at failure.

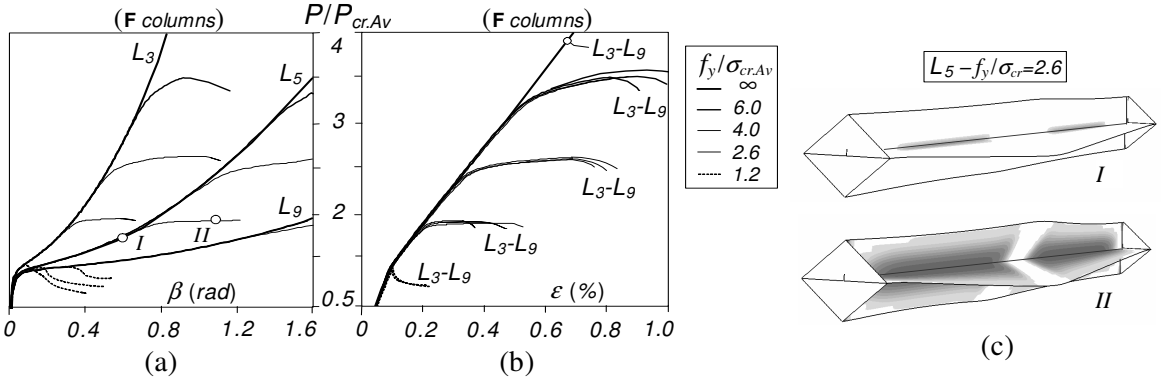

Figure 6: L_3, L_5, L_9 column (a) $P/P_{cr.Av}$ *vs.* β and (b) $P/P_{cr.Av}$ *vs.* ε paths ($5\,f_y/\sigma_{cr.Av}$), and (c) deformed configuration and plastic strain evolution ($L_5 + f_y/\sigma_{cr.Av}\approx 2.6$).

[4] Moreover, the shell finite element modeling of the fixed supports entails no stress concentrations.

Table 2: Variation of P_u (kN) with f_y for fixed columns.

Column	f_y (*MPa*)					
	235	*355*	*520*	*800*	*1200*	*1800*
L_3	*204*	*245*	*325*	*485*	*688*	*940*
L_4	*203*	*242*	*322*	*483*	*688*	*940*
L_5	*202*	*242*	*321*	*482*	*689*	*942*
L_6	*203*	*242*	*320*	*482*	*689*	*943*
L_7	*204*	*242*	*320*	*482*	*689*	*946*
L_8	*205*	*242*	*320*	*482*	*689*	*953*

(iv) Finally, a yield stress increase from *235* to *1800MPa* causes now a *470%* rise in column strength (from *≈200* to *≈950kN*) – this increase was about half (*225%*) in the pinned columns, reflecting the post-critical strength disparity between the columns exhibiting the two end support conditions.

4. Ultimate Strength and Design Considerations

Figs. 7(a)-(b) show the variation of the ultimate load ratio P_u/P_y (P_y is the squash load) with the slenderness $\overline{\lambda}=(f_y/\sigma_{cr})^{0.5}$ for the pinned (L_1-L_6) and fixed (L_3-L_8) columns. As for Fig. 7(c), it compares the cruciform column ultimate strength data gathered with a few experimental results reported by Nishimo *et al.* (1968) and Rasmussen & Hancock (1999), for fixed cruciform columns. Also included in Figs. 7(a)-(c) are the two current DSM (Direct Strength Method) "Winter-type" curves that provide estimates of column local and global ultimate strengths (*e.g.*, Schafer 2008)[5]. The joint observation of all these results makes it possible to conclude that:

(i) Since all pinned and fixed columns sharing the same yield stress have very similar ultimate strengths and critical stresses (the variation of σ_{cr} with L is minute – see Fig. 1(a)), the corresponding points

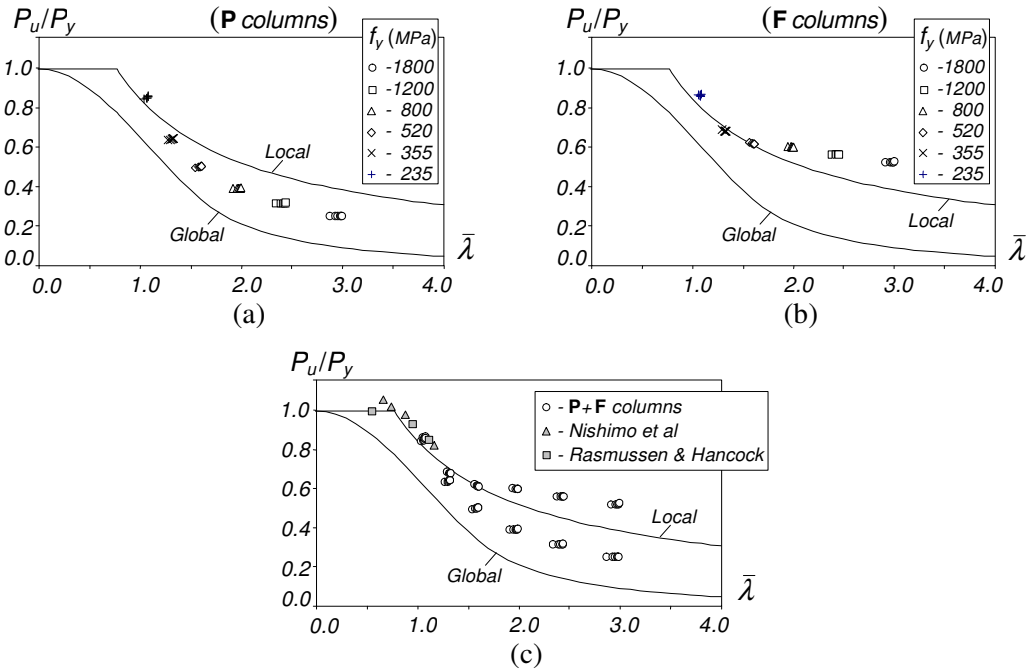

Figure 7: Variation of P_u/P_y with $\overline{\lambda}$: (a) pinned columns (numerical), (b) fixed columns (numerical) and (c) pinned and fixed columns (numerical) and fixed columns (experimental).

[5] Note that the DSM global column design curve was never calibrated against experimental or numerical ultimate strength values associated with pure torsional failures.

on the P_u/P_y vs. $\overline{\lambda}$ plan are almost coincident ("tightly grouped together") – their common slenderness obviously increases with the yield stress f_y.

(ii) Since columns with very similar torsional slenderness values have almost identical ultimate strengths, it seems fair to conclude that this slenderness constitutes an adequate (and convenient) "measure" to be used in the development of a design curve to predict the load-carrying capacity of short-to-intermediate pinned and fixed cruciform columns.

(iii) The qualitative and quantitative differences detected in the elastic post-buckling behaviors/strengths of the pinned and fixed columns become more pronounced (visible) as f_y increases. However, note that the pinned column ultimate strengths decrease significantly faster with $\overline{\lambda}$ than their fixed column counterparts – see Figs. 7(a)-(b).

(iv) The pinned column ultimate strengths remain fairly "aligned" with an ("imaginary") "Winter-type" curve located below the current DSM local design curve (see Fig. 7(a)) – for $\overline{\lambda} \geq 1.5$ (slender columns), the P_u/P_y values lie roughly half-way between the DSM local and global curves.

(v) As for the fixed column ultimate strengths, they (v_1) follow the DSM local design curve very closely up to $\overline{\lambda} \approx 1.5$ and (v_2) remain almost constant (quite small drops) for larger slenderness values (see Fig. 7(b)) – *i.e.*, this means that, relatively speaking, the ultimate strength rise is only slightly below the yield stress increase.

(vi) Fig. 7(c) clearly shows that a "spread" between the pinned and fixed column P_u/P_y values occurs for $\overline{\lambda} > 1.2$ and grows steadily with $\overline{\lambda}$. Finally, since all the experimental ultimate strengths reported by Nishimo *et al.* (1968) and Rasmussen & Hancock (1999) correspond to $\overline{\lambda} < 1.2$ (fairly stocky columns), it is not surprising that they are closely predicted by the DSM local design curve – no test results for higher slenderness values could be found in the literature.

5. Comparison with Angle Columns

In order to highlight the differences between the equal-leg angle and cruciform column post-buckling and strength behaviors, the numerical results presented and discussed above are now compared with those recently published by the authors (Dinis *et al.* 2010a) on the elastic and elastic-plastic post-buckling behavior and strength of pinned and fixed angle columns with (i) cross-section dimensions $70 \times 70mm$ and $t=1.2mm$, and (ii) short-to-intermediate lengths L_1-L_{11} ($20cm \leq L \leq 890cm$), corresponding to very similar critical buckling loads ("horizontal plateaus" of the P_{cr} *vs.* L curves). Note that a more detailed and mechanically-based comparison between the structural responses of these two types of columns will be reported in the near future (Dinis & Camotim 2011).

The main differences between the buckling, elastic post-buckling and elastic-plastic strength behaviors of angle and cruciform columns (both pinned and fixed) concern the following aspects:

(i) While all cruciform column "plateau" buckling loads correspond to pure torsional buckling, almost all their angle column counterparts are associated with either local-torsional (shorter lengths) or flexural-torsional (larger lengths) buckling – pure torsional buckling is just a "transition" between these two instability phenomena.

(ii) While the post-buckling response of all cruciform columns involves solely cross-section torsional rotations, the angle column post-buckling behavior is characterized by the simultaneous occurrence of cross-section torsional rotations and translations (corner displacements). The relative importance of the latter has a strong impact on the column post-buckling response, namely on its post-critical strength reserve and longitudinal normal stress distributions. Indeed, Figs. 8(a)-(b) and 9(a)-(b) show, respectively, the elastic (ii_1) P/P_{cr} *vs.* d/t (d is the mid-span corner displacement absolute

value) equilibrium paths concerning columns L_1-L_8 (pinned) and L_3-L_{11} (fixed), and (ii_2) mid-span normalized longitudinal normal stress (σ/σ_{cr}) evolution of columns L_3=53cm + L_5=133cm (pinned) and L_3=53cm + L_{10}=700cm (fixed). It is worth noting that, depending on the relevance of the corner displacements, which increases with the column length, the following aspects occur in both the pinned and fixed columns:

(ii.1) Two distinct sets of equilibrium paths can be identified: while (i_1) those concerning the shorter L_1-L_3 (pinned) and L_3-L_8 (fixed) columns, associated with very small corner displacements, are clearly stable and exhibit fairly high post-critical strengths, (i_2) the longer L_5-L_8 (pinned) and L_9-L_{11} (fixed) column ones, associated with significant corner displacements, always exhibit a limit point that is either "smooth" (mostly) or "abrupt" (L_9 and L_{10} fixed columns).

(ii.2) Two distinct mid-span longitudinal normal stress distribution evolutions, as post-buckling progresses, are also identified: while (ii_1) those concerning the shorter L_3 columns become either mildly asymmetric (pinned) or symmetric (fixed), (ii_2) the longer L_5 (pinned) and L_{10} (fixed) column stress distributions become markedly asymmetric.

(iii) Figs. 8(a)-(b) and 9(a)-(b) also clearly show that all the pinned and fixed angle column post-buckling deformations and longitudinal normal stress distributions differ from the "expected" ones (*e.g.*, Rasmussen 2005) – identical to those exhibited by a pair of pinned-free long plates. Indeed,

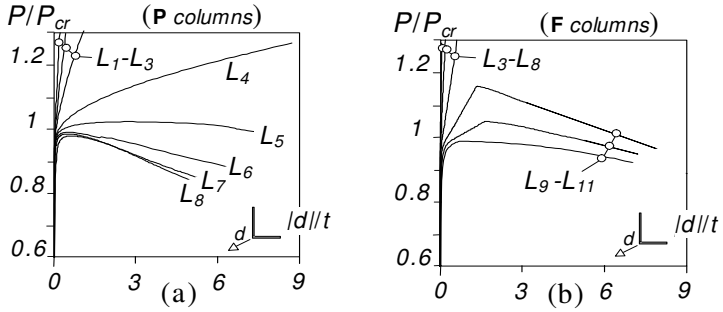

Figure 8: P/P_{cr} *vs. d/t* equilibrium paths for (a) pinned columns L_1-L_8 and (b) fixed columns L_3-L_{11} (Dinis *et al.* 2010a).

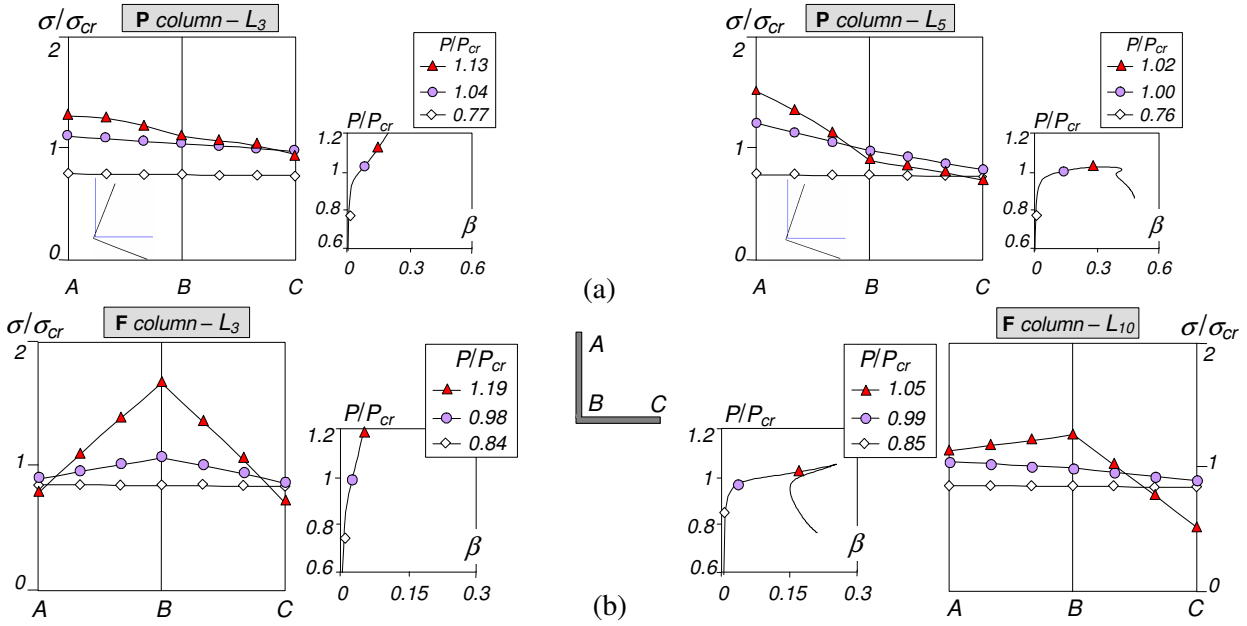

Figure 9: Mid-span normal stress distribution evolution: (a) L_3 + L_5 (pinned) and (b) L_3 + L_{10} (fixed) columns (Dinis *et al.* 2010a).

there are corner displacements (and not only cross-section torsional rotations) and the longitudinal normal stress distributions do not evolve towards parabolic diagrams (higher value at the corner). Note that these last features are also exhibited by the pinned and fixed cruciform columns analyzed in this work – they truly behave like four pinned-free long plates.

(iv) It was amply demonstrated by Dinis *et al.* (2010a) that the discrepancy between the determined and expected pinned and fixed angle column post-buckling behaviors stems from the occurrence of corner displacements, which invariably cause (more or less significant) bending, thus altering the longitudinal normal stress distributions. Indeed, by preventing the corner displacements it was possible to recover the (expected) pinned-free long plate post-buckling behavior. Note that, due to symmetry, no corner displacements occur in the pinned and fixed cruciform columns.

(v) While the ultimate strengths of all the pinned and fixed cruciform columns exhibiting very similar critical buckling stresses (but quite distinct lengths – corresponding to the "plateaus") and sharing a common yield stress are practically identical (see Figs. 7(a)-(b)), the same does not occur for the angle columns. Indeed, the ultimate strengths displayed in Figs. 10(a)-(b), taken from Dinis *et al.* (2010a) and obtained following the exact same approach adopted in this work, show that:

(v.1) While the pinned column values are moderately "packed together" (by no means as much as the pinned and fixed cruciform column ones – see Figs. 7(a)-(b)), those concerning the fixed columns exhibit a quite high "vertical dispersion", which implies a very significant variation of P_u/P_y with L (although the critical stress remains practically unaltered).

(v.2) The above assessment indicates that, unlike for cruciform columns, the critical slenderness is (v_1) only moderately adequate (pinned) or (v_2) completely inadequate (fixed) to predict angle column ultimate strengths. An alternative "measure", indispensable for fixed columns, is now being sought – the outcome of this search will be reported soon (Dinis *et al.* 2011).

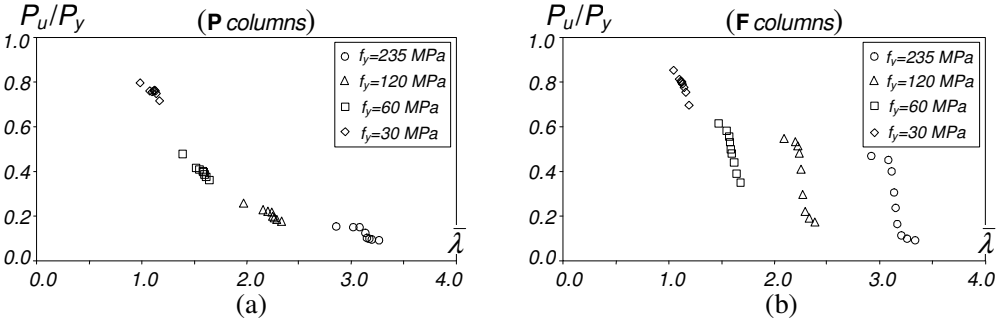

Figure 10: Variation of P_u/P_y with $\overline{\lambda}$ for (a) pinned and (b) fixed angle columns.

6. Conclusion

This paper reported the results of a numerical investigation on the buckling, post-buckling (elastic and elastic-plastic) and strength behavior of short-to-intermediate pinned and fixed cruciform steel columns. Although some GBT-based analyses were also carried out, aimed at clarifying the distinction between local and global buckling, most of these results were obtained through ABAQUS shell finite element analyses. They consisted of (i) elastic and elastic-plastic post-buckling equilibrium paths, and (ii) curves and diagrams showing the evolution, along a given path, of column deformations, normal stresses and plastic strains. The ultimate strengths obtained, together with a few experimental values available in the literature, were used to assess the quality of the estimates provided by the current Direct Strength Method design curves for local and global buckling. The paper closed with a brief comparison between the post-

buckling and strength behaviors of equal-leg angle and cruciform columns – this comparison was the original motivation of this work and will be further addressed in the near future (Dinis & Camotim 2011).

Among the various conclusions drawn from the numerical investigation reported in this paper, the following ones deserve to be specially mentioned:

(i) Both the pinned and fixed cruciform columns exhibit well defined critical stress "plateaus" that correspond almost exclusively to pure torsional buckling[6]. In angle columns, such "plateaus" involve either local-torsional or flexural-torsional buckling.

(ii) Inside the above "plateaus", both the pinned and fixed cruciform columns post-buckling behaviors are clearly stable (fairly high post-critical strength) and involve only cross-section torsional rotations. In particular, there are no corner displacements, which were recently found to play a crucial role in the post-buckling behavior and strength of angle columns (Dinis *et al.* 2010a).

(iii) The behavior of both the pinned and fixed cruciform columns can be viewed as the "sum" of four pinned-free long plates. In particular, the mid-span longitudinal normal stress distributions evolve towards the familiar parabolic diagrams obtained for the pinned-free long plates. Due to the corner displacements, angle columns are not the "sum" of two pinned-free long plates – *e.g.*, the mid-span longitudinal normal stress distributions become far from parabolic as post-buckling progresses.

(iv) Within the length range under consideration, the results obtained appear to indicate that the critical slenderness provides an adequate "measure" to estimate the cruciform column ultimate strength – the columns sharing the same $\overline{\lambda}$ value have practically identical load-carrying capacities. In angle columns, this critical slenderness was found to be either moderately adequate (pinned columns) or completely inadequate (fixed columns) to predict the ultimate strength (Dinis *et al.* 2010a).

(v) The numerical ultimate strength values obtained in this work either (v_1) lie in between the existing DSM local and global design curves (pinned columns)[7] or (v_2) are safely predicted by the DSM local design curve (fixed columns) – excessively so for $\overline{\lambda} \geq 1.5$. The available experimental results, all concerning stocky fixed columns are in perfect agreement with these findings.

References

Chen G, Trahair NS (1994). "Inelastic torsional buckling strengths of cruciform columns", *Engineering Structures*, 16(2), 83-90.

Chodraui GMB, Shifferaw Y, Malite M, Schafer BW (2007). "On the stability of cold-formed steel angles under compression", REM – Revista Escola de Minas (Brazil), **60**(2), 355-363. (Portuguese).

Dabrowsi R (1988). "On torsional stability of cruciform columns", *Journal of Constructional Steel Research*, **9**(1), 51-59.

Dinis PB, Camotim D (2006). "On the use of shell finite element analysis to assess the local buckling and post-buckling behaviour of cold-formed steel thin-walled members", *Abstracts of III European Conference on Computational Mechanics: Solids, Structures and Coupled Problems in Engineering* (III ECCM – Lisboa, 5-9/6), C.A.M. Soares *et al.* (eds.), Springer, 689. (full paper in CD-ROM Proceedings)

Dinis PB, Camotim D (2011), "Buckling, post-buckling and strength of equal-leg angle and cruciform columns: similarities and differences", *Proceedings of the Sixth European Conference on Steel and Composite Structures* (EUROSTEEL 2011 – Budapest, 31/8-2/9), in press.

Dinis PB, Camotim D, Silvestre N (2007). "FEM-based analysis of the local-plate/distortional mode interaction in cold-formed steel lipped channel columns", *Computers & Structures*, **85**(19-20), 1461-1474.

Dinis PB, Camotim D, Silvestre N (2008). "On the local and global buckling behaviour of angle, T-section and cruciform thin-walled columns and beams", *Proceedings of Fifth International Conference on Coupled Instabilities in Metal Structures* (CIMS 2008 – Sydney, 23-24/6), K. Rasmussen, T. Wilkinson (eds.), 281-290.

[6] The fixed column results apply also to columns with their end cross-sections attached to rigid end-plates that are free to exhibit flexural rotations – columns often termed "simply supported" in the literature.

[7] With the exception of the stockier columns ($\overline{\lambda} \approx 1.0$), whose ultimate strengths lie slightly above the DSM local design curve.

Dinis PB, Camotim D, Silvestre N (2010a). "Post-buckling behaviour and strength of angle columns", *Proceedings of International Colloquium on Stability and Ductility of Steel Structures* (SDSS'2010 – Rio de Janeiro, 8-10/9), E. Batista, P. Vellasco, L. Lima (eds.), 1141-1150 (vol. 2).

Dinis PB, Camotim D, Silvestre N (2010b). "On the local and global buckling behaviour of angle, T-section and cruciform thin-walled members", *Thin-Walled Structures*, **48**(10-11), 786-797.

Dinis PB, Camotim D, Silvestre N (2011). "On the design of cold-formed steel angle columns", *Proceedings of the Sixth International Conference on Thin-Walled Structures* (ICTWS 2011 – Timisora, 5-7/9), in press.

Ellobody E, Young B (2005). "Behavior of cold-formed steel plain angle columns", *Journal of Structural Engineering* (ASCE), **131**(3), 457-466.

Kitipornchai S, Chan SL (1987). "Nonlinear finite-element analysis of angle and tee beam-columns", *Journal of Structural Engineering* (ASCE), **113**(4), 721-739.

Mohan SJ, Rao NP, Lakshmanan N (2005). "Flexural and local buckling interaction of steel angles", *International Journal of Structural Stability and Dynamics*, **5**(2), 143-162.

Kitipornchai S, Albermani FGA, Chan SL (1990). "Elastoplastic finite-element models for angle steel frames", *Journal of Structural Engineering* (ASCE), **116**(10), 2567-2581.

Nishimo F, Tall L, Okumura T (1968). "Residual stress and torsional buckling strength of H and cruciform columns", *Transactions of the Japanese Society of Civil Engineers* (JSCE), **160** (December), 57-87.

Popovic D, Hancock GJ, Rasmussen KJR (1999). "Axial compression tests of cold-formed angles", *Journal of Structural Engineering* (ASCE), **125**(5), 515-523.

Popovic D, Hancock GJ, Rasmussen KJR (2001). "Compression tests on cold-formed angles loaded parallel with a leg", *Journal of Structural Engineering* (ASCE), **127**(6), 600-607.

Rasmussen KJR (2005). "Design of angle columns with locally unstable legs", *Journal of Structural Engineering* (ASCE), **131**(10), 1553-1560.

Rasmussen KJR (2006). "Design of slender angle section beam-columns by the direct strength method", *Journal of Structural Engineering* (ASCE), **132**(2), 204-211.

Rasmussen KJR, Hancock GJ (1992). "Plate slenderness limits for high strength steel sections", *Journal of Constructional Steel Research*, **23**(1-3), 73-96.

Schafer BW (2008). "Review: the direct strength method of cold-formed steel member design", *Journal of Constructional Steel Research*, **64**(7-8), 766-778.

Simulia Inc. (2008). *Abaqus Standard* (vrs. 6.7-5).

Stowell EZ (1951). "Compressive strength of flanges", National Advisory Committee for Aeronautics (NACA) Report nº 1029.

Trahair N.S. (2003). "Lateral buckling strength of steel angle section beams", *Journal of Structural Engineering* (ASCE), 129(6), 784-791.

Trahair NS (2005). "Buckling and torsion of steel unequal angle beams", *Journal of Structural Engineering* (ASCE), **131**(3), 474-480.

Young B, Ellobody E (2007). "Design of cold-formed steel unequal angle compression members", *Thin-Walled Structures*, **45**(3), 330-338.

Young B (2004). "Tests and design of fixed-ended cold-formed steel plain angle columns", *Journal of Structural Engineering* (ASCE), **130**(12), 1931-1940.